Slip-weakening distance estimated at near-fault stations

Eiichi Fukuyama[1] and Takeshi Mikumo[2,3]

Received 25 December 2006; revised 17 March 2007; accepted 28 March 2007; published 1 May 2007.

[1] We estimated the slip-weakening distance from the seismograms recorded at near-fault stations, considering the effect of spatio-temporal filtering for a continuous propagation of rupture. This effect is usually observed at some distance away from the fault. We used a Green's function for 2-D anti-plane rupture propagating with constant rupture velocity and instantaneous slip at the crack tip. As a source time function, we used a regularized Yoffe function which is a kinematically good approximation of dynamic slip-weakening behavior. By convolving these functions, near-fault waveforms are computed. As a proxy of slip-weakening distance (D_c), we used D_c', which is defined as a slip at the time of peak slip velocity. Then, D_c' values can be computed as a function of the distance from the fault. This procedure is applied to the observation of the 2000 western Tottori, Japan, earthquake (M_W6.6) as well as the 2002 Denali, Alaska, earthquake (M_W7.9). We estimated D_c' at about 0.3 m at GSH station (~100 m away from the fault) for the Tottori earthquake and that at about 2.5 m at PS10 station (~3 km away from the fault) for the Denali earthquake. We confirmed that both estimates are not affected by the spatio-temporal smoothing. **Citation:** Fukuyama, E., and T. Mikumo (2007), Slip-weakening distance estimated at near-fault stations, *Geophys. Res. Lett.*, *34*, L09302, doi:10.1029/2006GL029203.

1. Introduction

[2] Slip-weakening distance (D_c) is one of the important parameters to describe the dynamic fault rupture process. *Ida* [1972] proposed an idea of slip-weakening behavior at crack tip by considering the energy budget. Then *Ohnaka et al.* [1987] and *Okubo* [1989] showed the existence of this feature in the laboratory. *Matsu'ura et al.* [1992] convincingly explained the physical background of this slip-weakening behavior. More recently, *Bizzarri et al.* [2001] demonstrated that this feature exists at high slip velocities even under the rate- and state friction law proposed by *Dieterich* [1984].

[3] Although the slip-weakening distance has been measured in the laboratory, we still did not know how large it is for real earthquakes. To constrain the numerical simulation models as well as the laboratory experiments, it is undoubtedly necessary to obtain the slip-weakening distance for real earthquakes without uncertainties.

[4] *Ide and Takeo* [1997] estimated the slip-weakening distance for the 1995 Kobe earthquake as 0.5–1.0 m. However, it is possible that this estimate could be biased when solving dynamic rupture propagation. *Piatanesi et al.* [2004] pointed out that the estimation of D_c depends on the shape of source time function assumed for kinematic source modeling. They suggested that a slight change of its shape could affect the estimate of slip-weakening distance when generating very similar seismic waves at distance.

[5] To overcome this situation, *Mikumo et al.* [2003] proposed a technique to estimate a slip-weakening distance more directly from seismic observation. They proposed D_c' value as a proxy of D_c,which is defined as a slip at the time of peak slip velocity. As noted by *Fukuyama et al.* [2003b], this approximation works well, as far as the rupture propagates smoothly. On the other hand, *Spudich and Guatteri* [2004] and *Yasuda et al.* [2005] pointed out that the spatio-temporal smoothing effects still make the estimation of D_c biased.

[6] In the present paper, we discuss the applicability of the D_c' technique to the near-fault seismograms by taking into account the spatio-temporal smoothing effect. After the examination of this effect, we estimated the slip-weakening distance during two strike-slip earthquakes from D_c' directly measured with near-fault seismograms.

2. Method for D_c Evaluation

[7] Although there are several formulations for the kinematic expression of the source time function [e.g., *Nakamura and Miyatake*, 2000], we use here the regularized Yoffe function [*Tinti et al.*, 2005], because it is defined by only 3 independent parameters that are directly related to the dynamic parameters and is a good approximation for the slip-weakening rupture model [*Tinti et al.*, 2005]. The regularized Yoffe function can be given by the following equation.

$$s(x,t) = D\int_{-\infty}^{+\infty} Y(x,\tau)W(t-\tau)d\tau \qquad (1)$$

where D is the final slip. x is the distance along the fault. $Y(x, t)$ and $W(t)$ are the original Yoffe function and a triangular function, respectively and can be expressed as follows.

$$Y(x,t) = \frac{2}{\pi\tau_R}H(t')H(\tau_R - t')\sqrt{\frac{\tau_R - t'}{t'}}$$
$$W(t) = \frac{1}{\tau_S^2}[tH(t)H(\tau_s - t) + (2\tau_S - t)H(t-\tau_S)H(2\tau_s - t)]$$

where $t' = t - t_0(x)$, $t_0(x)$ is the rupture time at x, τ_R is the rise time for the Yoffe function and τ_S is the smoothing

[1]National Research Institute for Earth Science and Disaster Prevention, Tsukuba, Japan.
[2]Instituto de Geofisica, Universidad Nacional Autonoma de Mexico, Mexico D. F., Mexico.
[3]Retired.

0094-8276/07/2006GL029203

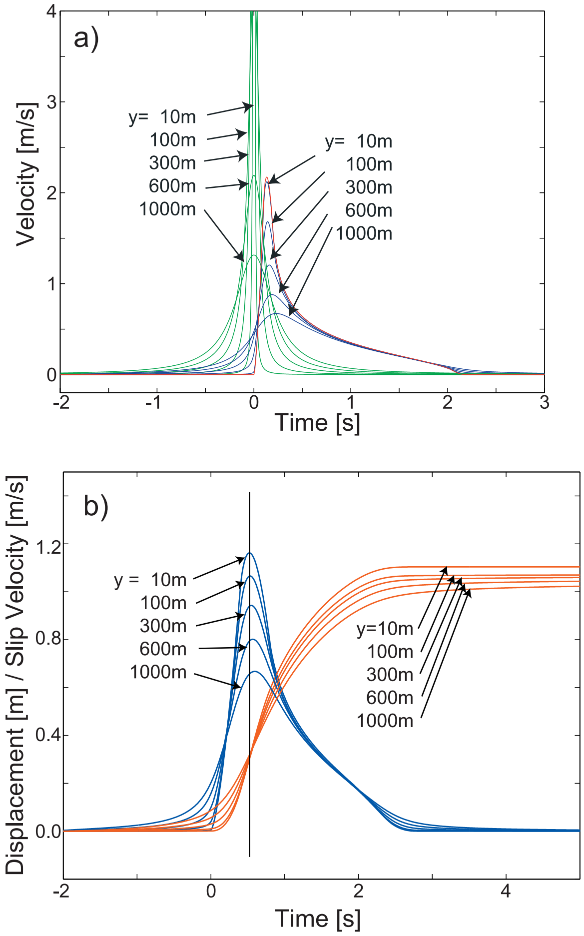

Figure 1. (a) Source time function (red), fault-parallel component Green's function at distances 10 m, 100 m, 300 m, 600 m, and 1000 m from the fault (green) and the corresponding synthetic seismograms (blue) obtained by convolving the source time function. (b) Velocity seismograms (blue) and displacements (red) plotted for several distances away from the fault. All velocity seismograms are approximately aligned for the peak velocity time. The displacements at the time of peak velocity are considered as D_c'.

constant which is approximated by the parameter T_{acc}, the time to the peak slip velocity [*Tinti et al.*, 2005]. According to *Tinti et al.* [2005], the relation $T_{acc} = 1.3\ \tau_S$ is obtained.

[8] As a Green's function, we used a 2-D anti-plane rupture model where the rupture propagates with constant rupture velocity and a slip occurs instantaneously at the crack tip [*Aki and Richards*, 2002, chapter 10.2]. This Green's function has the same form as that propagating with shear wave velocity for the in-plane rupture. The Green's function in this case can be written as follows.

$$g(x,y,t) = \frac{v}{2\pi} \frac{\sqrt{1 - v^2/\beta^2}}{(x - vt)^2 + (1 - v^2/\beta^2)y^2} y \qquad (2)$$

where β is S-wave velocity and v is the rupture velocity. y is the distance perpendicular to the fault. Since we wanted to focus on the spatio-temporal effect for off-fault observation, we used the simplest Green's function.

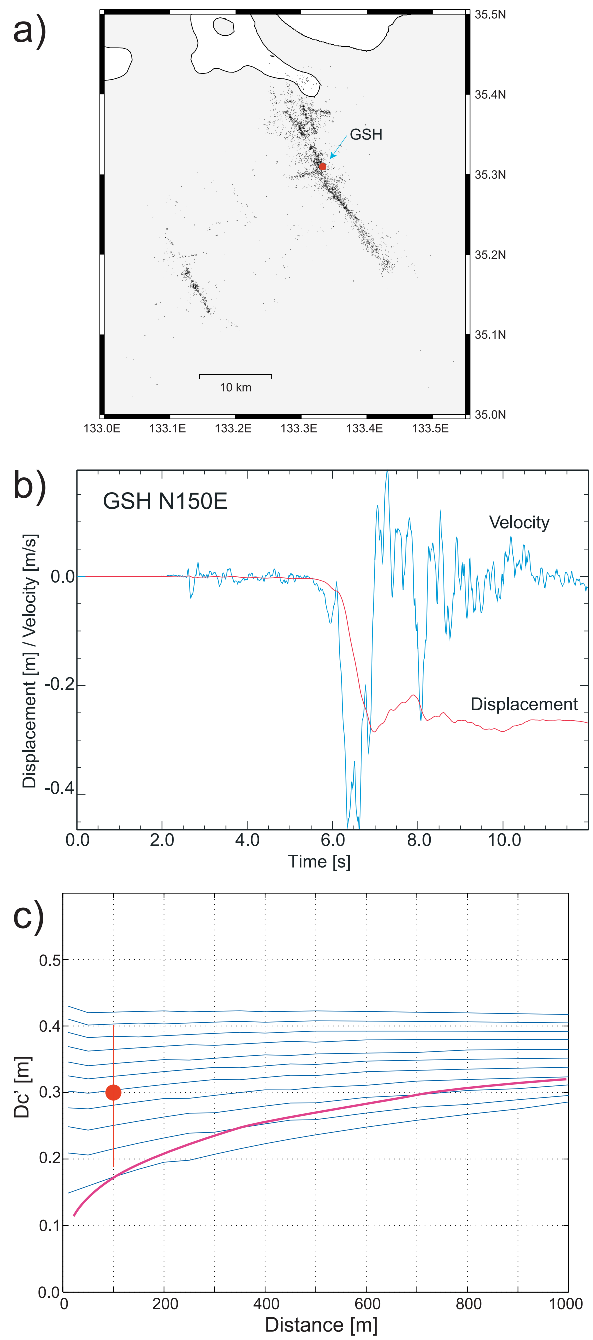

Figure 2. (a) Location of the GSH station (red circle) plotted with the aftershock distribution of the 2000 western Tottori earthquake. (b) Fault parallel component of the observed velocity (blue) and displacement (red) seismograms, which are obtained from the numerical integration of the original accelerograms. (c) Simulated D_c' values (blue curves) for different sets of assumed D_c values plotted as a function of distance from the fault for the 2000 western Tottori earthquake. Red thick curve indicates the lower bound of the area below which the estimation error of D_c' is greater than 20%. Red circle indicates the measured D_c' at the GSH station and vertical line shows its uncertainty.

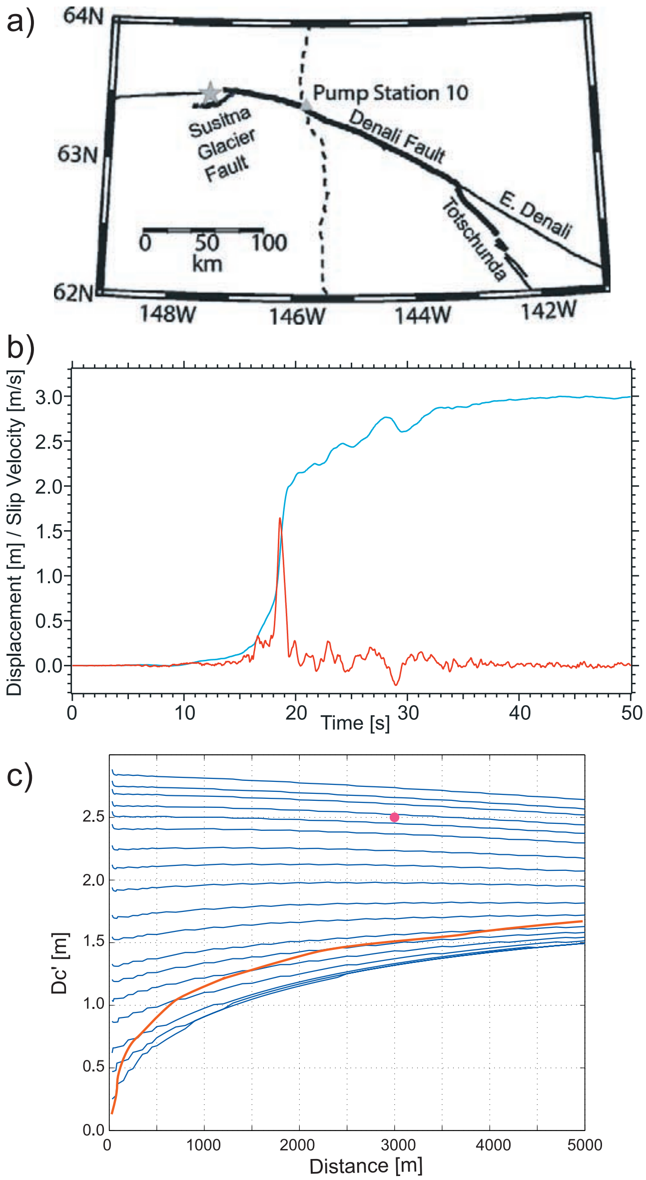

Figure 3. (a) Location of PS10 (Pump Station 10) shown with the fault trace of the Denali earthquake [after *Ellsworth et al.*, 2004]. (b) Fault parallel component of the observed ground velocity (blue) and ground displacement (red) at PS10, which were provided by *Ellsworth et al.* [2004] (used with permission from EERI). (c) Simulated D_c' values (blue curves) for different sets of assumed D_c values plotted as a function of distance from the fault for the 2002 Denali earthquake. Red thick curve indicates the lower bound of the area below which the estimation error of D_c' is greater than 20%. Red circle shows the measured D_c' at the PS10 station.

[9] Then, near-fault displacement can be obtained by convolving the above two functions.

$$u(x, y, t) = \int s(x, \tau) g(x, y, t - \tau) d\tau \tag{3}$$

This means that the synthetic waveform can be obtained as a function of v, τ_R, D, y and τ_S. As shown by *Tinti et al.* [2005], $\tau_S \propto T_{acc} \propto D_c/\Delta\tau_b$, where $\Delta\tau_b$ is the critical strength drop. Thus, the real slip-weakening distance D_c is implicitly related to τ_S.

[10] Therefore, once we know v, τ_R, and D from the waveform inversion results, the synthetic waveforms can be computed for various values of D_c as a function of y. Then from these synthetic seismograms, variation of D_c' as a function of y can be obtained by measuring the amount of slip at the time of peak slip velocity in each seismogram. Then, finally, we evaluate the range of y as a function of D_c where D_c can be estimated uniquely and reasonably well approximated by D_c' estimation.

[11] From Figure 1a, we see that the effect of spatio-temporal smoothing becomes significant by looking at the broadening of the pulse width in Green's functions at distances. Since the Green's function here is the waveform caused by an impulsive slip velocity time function, we expect that for shorter D_c cases, this spatio-temporal effect would become crucial. In these cases, D_c' tends to be overestimated when the station is located far away from the fault. In contrast, for larger D_c, the spatio-temporal effect may be negligible and we are able to estimate D_c' at near-fault stations slightly far away. In addition, from Figure 1b, it should be noted that the estimate of D_c', which is slip at the time of peak slip velocity, is rather robust and we expect that this technique works practically well.

3. Application to the Observation

3.1. The 2000 Western Tottori Earthquake

[12] We first applied the above technique to the 2000 western Tottori earthquake (M_w6.6). This is one of the best investigated earthquakes because it occurred after the installation of very dense high-quality nation-wide seismic networks in Japan (Hi-net, F-net, K-net and Kik-net) [e.g., *Fukuyama et al.*, 2003a].

[13] In the source region of the 2000 western Tottori earthquake, an accelerometer had been installed and operated by the local government of Tottori Prefecture at the bottom of the bank of the Kasho dam (GSH, 35.30888°N, 133.32944°E, 0.07 km in height) (Figure 2a), and was able to record the ground motion of this earthquake. The location

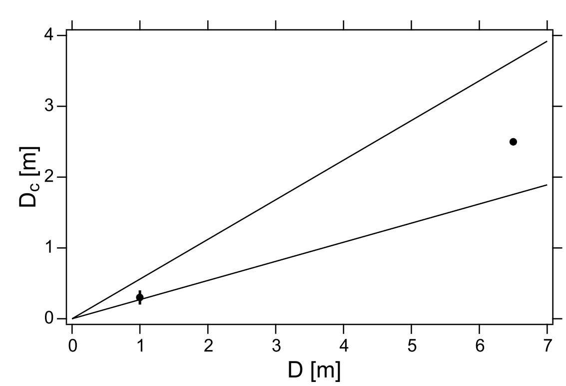

Figure 4. Two solid circles indicating the results of estimated D_c for the western Tottori and Denali earthquakes plotted as a function of total slip (D). Two solid lines stand for the upper and lower limits of D_c (D_c = 0.56 D and D_c = 0.27 D, respectively) estimated by *Mikumo et al.* [2003].

of GSH station is estimated at about 100 m east of the fault trace. We measured the orientation of the seismograph by a gyrocompass and found that the nominal north direction was N7°W. Taking into account this information, we reproduced the fault parallel ground velocity and displacement as shown in Figure 2b by integrating the observed accelerograms.

[14] We measured the D_c' by picking the time of peak ground velocity, following *Mikumo et al.* [2003]. Since this earthquake was of strike slip type, slip on the fault should be considered as twice the displacement on either side of the fault. From Figure 2b, two velocity peaks are observed, each of which corresponds to D_c' = 0.2 m and 0.4m. Since these two split peaks seem to be caused by the local structure, we estimated a mean value of D_c' as about 0.3 m.

[15] From the waveform inversion results [*Iwata and Sekiguchi*, 2002], the rupture velocity v is estimated at 2.8 km/s, rise time τ_R is 2 s and total slip D is 1 m. Assuming these values, synthetic seismograms are computed for various τ_S and y. Then, D_c' is measured from the synthetic seismograms and the relation between D_c' and y is obtained. as shown in Figure 2c. The red curve stands for the lower bounds of reliable range of D_c estimation, with the 20% error. The 20% error corresponds to a typical estimation error of D_c' [*Mikumo et al.*, 2003]. Since the present estimation of 0.3 m for D_c at GSH for the western Tottori earthquake is inside this area, our estimation would not be affected by the spatio-temporal smoothing.

[16] Although there appeared clear fault lineaments from the aftershock distribution [*Fukuyama et al.*, 2003a] and the existence of shallow fault slip was estimated from the geodetic data inversion [*Sagiya et al.*, 2002], no obvious surface fault break appeared during this earthquake. Therefore the estimation error of D_c' might be larger than predicted.

3.2. The 2002 Denali Earthquake

[17] The 2002 Denali earthquake occurred on November 3, 2002 with 340 km surface rupture along the Denali and related faults [e.g., *Eberhart-Phillips et al.*, 2003]. A set of near-fault seismograms was obtained 3 km away from the fault at Pump Station 10 (PS10, 63.4244944°N, 145.762664°W, 0.7261 km in height) (Figure 3a) by the Alyeska Pipeline Service Company [*Ellsworth et al.*, 2004].

[18] *Ellsworth et al.* [2004] carefully investigated these seismograms, especially, the orientation of seismometer and the characteristics of high-pass filtering, and they obtained the corrected ground velocity and displacement (Figure 3b). We employed these seismograms for the estimation of D_c'. From Figure 3b, we measured that D_c' is about 2.5 m, which is obtained as twice the displacement at the time of peak slip velocity in the fault-parallel component.

[19] We evaluated the spatio-temporal smoothing effect in the same way as above. In the present case, we used the following parameters: 6.5 m for the slip displacement D, 3.4 km/s for the rupture velocity v and 5.0 s for the rise time τ_R, which are taken from the kinematic waveform inversion by *Dreger et al.* [2004] and *Oglesby et al.* [2004]. The obtained results are shown in Figure 3c. The decrease in D_c' for large D_c as a function of y in Figure 3c is caused by the geometrical spreading effect. From Figure 3c, we could confirm that the spatio-temporal effect is negligible even if the station PS10 is located 3 km away from the fault trace.

4. Conclusions

[20] We have proposed a method to qualify the slip-weakening distance estimated from near-fault seismograms by taking into account the spatio-temporal smoothing effect. Synthetic simulations with the regularized Yoffe function are conducted to clarify its influence. Then, we applied this method to the observed near-fault seismograms obtained during the 2000 western Tottori (M_W6.6) and the 2002 Denali (M_W7.9) earthquakes.

[21] From these simulations we confirmed that the obtained D_c' values for both of the western Tottori and Denali earthquakes are significant and that these values estimated from the observed records are not significantly affected by the spatio-temporal effects. The estimated D_c' values are 0.3 m for the western Tottori and 2.5 m for the Denali earthquakes. We plot these values in Figure 4 comparing with those obtained by *Mikumo et al.* [2003] and found that our estimates fall between the range of the previous estimates, indicating consistent results.

[22] **Acknowledgments.** We thank the local government of the Tottori prefecture for the permission to use the seismograms at Kasho dam. We also thank Bill Ellsworth for making the seismogram at PS10 available. Comments by two anonymous reviewers were very helpful to improve the manuscript.

References

Aki, K., and P. G. Richards (2002), *Quantitative Seismology*, 2nd ed., 700 pp., Univ. Sci., Sausalito, Calif.
Bizzarri, A., M. Cocco, D. J. Andrews, and E. Boschi (2001), Solving the dynamic rupture problem with different numerical approaches and constitutive laws, *Geophys. J. Int.*, *144*, 656–678.
Dieterich, J. H. (1984), A model for the nucleation of earthquake slip, in *Earthquake Source Mechanics*, *Geophys. Monogr. Ser.*, vol. 37, edited by S. Das, J. Boatwright, and C. H. Scholz, pp. 37–47, AGU, Washington, D. C.
Dreger, D. S., D. D. Oglesby, R. Harris, N. Ratchkovski, and R. Hansen (2004), Kinematic and dynamic rupture models of the November 3, 2002 Mw7.9 Denali, Alaska, earthquake, *Geophys. Res. Lett.*, *31*, L04605, doi:10.1029/2003GL018333.
Eberhart-Phillips, D., et al. (2003), The 2002 Denali fault earthquake, Alaska: A large magnitude, slip-partitioned event, *Science*, *300*, 1113–1118.
Ellsworth, W. L., M. Celebi, J. R. Evans, E. G. Jensen, R. Kayen, M. C. Metz, D. J. Nyman, J. W. Roddick, P. Spudich, and C. D. Stephens (2004), Near-field ground motion of the 2002 Denali fault, Alaska, earthquake recorded at pump station 10, *Earthquake Spectra*, *20*, 597–615.
Fukuyama, E., W. L. Ellsworth, F. Waldhauser, and A. Kubo (2003a), Detailed fault structure of the 2000 western Tottori, Japan, earthquake sequence, *Bull. Seismol. Soc. Am.*, *93*, 1468–1478.
Fukuyama, E., T. Mikumo, and K. B. Olsen (2003b), Estimation of the critical slip-weakening distance: Theoretical background, *Bull. Seismol. Soc. Am.*, *93*, 1835–1840.
Ida, Y. (1972), Cohesive force on longitudinal crack and Griffith's specific surface energy, *J. Geophys. Res.*, *77*, 3796–3805.
Ide, S., and M. Takeo (1997), Determination of constitutive relations of fault slip based on seismic wave analysis, *J. Geophys. Res.*, *102*, 27,379–27,391.
Iwata, T., and H. Sekiguchi (2002), Source process and near-source ground motion during the 2000 Tottori-ken Seibu earthquake (Mw6.8), in *Reports on Assessments of Seismic Local-site Effects at Plural Test Sites*, edited by K. Kudo. pp. 231–241, Min. of Educ., Cult., Sports, Sci., and Technol., Tokyo.
Matsu'ura, M., H. Kataoka, and B. Shibazaki (1992), Slip-dependent friction law and nucleation processes in earthquake rupture, *Tectonophysics*, *211*, 135–148.
Mikumo, T., K. B. Olsen, E. Fukuyama, and Y. Yagi (2003), Stress-breakdown time and slip-weakening distance inferred from slip-velocity functions on earthquake faults, *Bull. Seismol. Soc. Am.*, *93*, 264–282.
Nakamura, H., and T. Miyatake (2000), An approximate expression of slip velocity time function for simulation of near-field strong ground motion (in Japanese with English abstract), *J. Seismol. Soc. Jpn.*, *53*, 1–9.

Oglesby, D. D., D. S. Dreger, R. A. Harris, N. Ratchkovski, and R. Hansen (2004), Inverse kinematic and forward dynamic models of the 2002 Denali fault earthquake, Alaska, *Bull. Seismol. Soc. Am.*, *94*, S214–S233.
Ohnaka, M., Y. Kuwahara, and K. Yamamoto (1987), Constitutive relations between dynamic physical parameters near a tip of the propagating slip zone during stick-slip shear failure, *Tectonophysics*, *144*, 109–125.
Okubo, P. G. (1989), Dynamic rupture modelling with laboratory-derived constitutive relations, *J. Geophys. Res.*, *94*, 12,321–12,335.
Piatanesi, A., E. Tinti, M. Cocco, and E. Fukuyama (2004), The dependence of traction evolution on the earthquake source time function adopted in kinematic rupture models, *Geophys. Res. Lett.*, *31*, L04609, doi:10.1029/2003GL019225.
Sagiya, T., T. Nishimura, Y. Hatanaka, E. Fukuyama, and W. L. Ellsworth (2002), Crustal movements associated with the 2000 western Tottori earthquake and its fault models (in Japanese with English abstract), *J. Seismol. Soc. Jpn.*, *54*, 523–534.
Spudich, P., and M. Guatteri (2004), The effect of bandwidth limitations on the inference of earthquake slip-weakening distance from seismograms, *Bull. Seismol. Soc. Am.*, *94*, 2028–2036.
Tinti, E., E. Fukuyama, A. Piatanesi, and M. Cocco (2005), A kinematic source-time function compatible with earthquake dynamics, *Bull. Seismol. Soc. Am.*, *95*, 1211–1223.
Yasuda, T., Y. Yagi, T. Mikumo, and T. Miyatake (2005), A comparison between D_c'-values obtained from a dynamic rupture model and waveform inversion, *Geophys. Res. Lett.*, *32*, L14316, doi:10.1029/2005GL023114.

E. Fukuyama, National Research Institute for Earth Science and Disaster Prevention, Tsukuba, Ibaraki 305-0006, Japan. (fuku@bosai.go.jp)
T. Mikumo, 39-809 Kohata-Okurayama, Uji, Kyoto, Japan. (mikumo@maia.eonet.ne.jp)